Available online at www.sciencedirect.com
ScienceDirect
ELSEVIER
Polymer 47 (2006) 6293–6302
polymer
www.elsevier.com/locate/polymer

Effect of copolymer composition on acid-catalyzed deprotection reaction kinetics in model photoresists ☆

Shuhui H. Kang [a], Vivek M. Prabhu [a,*], Bryan D. Vogt [a], Eric K. Lin [a], Wen-li Wu [a], Karen Turnquest [b]

[a] Polymers Division, National Institute of Standards and Technology (NIST), 100 Bureau Drive, Gaithersburg, MD 20899, United States
[b] SEMATECH, 2706 Montopolis Drive, Austin, TX 78741, United States

Received 26 April 2006; received in revised form 30 June 2006; accepted 3 July 2006
Available online 25 July 2006

Abstract

The kinetics of the deprotection reaction in model photoresist materials was measured as a function of copolymer composition with Fourier transform infrared (FTIR) spectroscopy. A mathematical model was developed to analyze the deprotection kinetics in terms of the coupled reaction rate and acid-diffusion processes. The first-order reaction rate constant decreases as the non-reactive comonomer content increased. Additionally, the extent of reaction appears to saturate to different levels as a function of reaction temperature. The resulting composition-dependent reaction constant arises from a dramatically reduced acid transport rate due to a strong interaction of the acid with the increasing polar resist matrix. The reduced acid transport is consistent with the observed hydrogen bonding between the photoacid and methacrylic acid reaction product. These results provide important insight into the effect of the changing polymer composition on the acid-catalyzed reaction kinetics.
© 2006 Elsevier Ltd. All rights reserved.

Keywords: Photoresist; Photoacid; Reaction-diffusion

1. Introduction

Chemically amplified photoresists are the predominant materials used in the fabrication of nanoscale structures with photolithography. In this process, patterns are delineated chemically through the production of acid in areas exposed through a mask and an acid-catalyzed deprotection reaction that changes the solubility of the reacted material in an aqueous base solution [1]. The patterning process is complex because the reaction is catalyzed by a diffusing acid species during a post-exposure bake. The reaction-diffusion process, while following known chemical reactions, can be difficult to control and optimize because the spatial extent of reaction and the reaction kinetics are affected by the concentration and diffusion of the acid as well as by a dynamically changing matrix composition that in turn modifies the acid transport processes [2]. High resolution features with ever decreasing sizes have been produced by tuning any number of process and material characteristics including the photoresist formulation and the polymer chemistry or composition.

These coupled processes have been investigated through fundamental studies to identify the leading factors that affect chemically amplified photoresist performance. Postnikov et al. [3] studied photoacid diffusion in a simplified model system and observed that photoacid transport within a reactive polymer does not follow Fickian diffusion. In order to understand the spatial extent of this photoacid-catalyzed reaction front, Lin et al. confirmed the non-Fickian shape by neutron and X-ray reflectivity [4]. However, the performance of actual photoresist systems requires recognition of the spatial heterogeneity of the reaction-diffusion process that arises from the discrete concentration of the acid and the local composition of the material. Schmid et al. [5] used mesoscale simulations to understand the role of photoacid distribution on this heterogeneity. They concluded that the contrast between regions of

☆ Official contribution of the National Institute of Standards and Technology; not subject to copyright in the United States.

* Corresponding author. Tel.: +1 301 975 3657; fax: +1 301 975 3928.
E-mail address: vprabhu@nist.gov (V.M. Prabhu).

0032-3861/$ - see front matter © 2006 Elsevier Ltd. All rights reserved.
doi:10.1016/j.polymer.2006.07.003

high versus low photoacid concentrations was needed to minimize the deprotection gradient to enable sharper image profiles. The results from these simulations were consistent with data from the interferometric lithographic studies of Hinsberg et al. [6]. Houle et al. analyzed the chemical equilibrium of the deprotection reaction with the photoacid (hopping) transport through simulation and experiment [2]. They predicted that the extent of reaction in the photoresist becomes self-limited due to disparate diffusion coefficients in protected versus deprotected regions. Such local heterogeneity becomes even more complex when introducing non-reactive moieties, base-quenching species [7,8], or systems where the miscibility of the component materials is questionable [9]. To date, there are few systematic studies on the effect of the photoresist polymer composition on the reaction-diffusion process.

In this paper, we quantify the effect of copolymer composition on the reaction-diffusion process in a model photoresist system using Fourier transform infrared (FTIR) spectroscopy and a mathematical model. Through changes in the apparent reaction rate constant, we find that increasing fractions of non-reacting comonomer reduce the photoacid transport rate; as the extent of the deprotection reaction increases, the products effectively trap the photoacid and subsequently slow down the observed reaction kinetics. To describe the experimental data, a chemical-specific photoacid trapping term is needed in the mathematical model and leads to an additional acid-trapping rate constant. The FTIR data also show that the reduced acid-diffusion rate is a result of hydrogen bonding between the photoacid and the reaction product. The mathematical model and the experimental data are fully consistent, providing a quantitative measure of the influence of the polymer composition on the reaction and diffusion processes. This information provides the foundation to quantitatively understand the balance between the deprotection reaction propagation and termination (trapped acid) and to investigate further the complexity of the deprotection profile shape and heterogeneity [10].

2. Experimental[1]

2.1. Polymer characteristics

Poly(methyladamantyl methacrylate) (PMAdMA) and poly(methyladamantyl methacrylate-*co*-α-gammabutyrolactone methacrylate), containing 59 mol% α-gammabutyrolactone methacrylate were provided by DuPont Electronics Polymers. The second copolymer containing 50 mol% α-gammabutyrolactone methacrylate (P(MAdMA$_{50}$-*co*-GBLMA$_{50}$)) was supplied by AZ Electronics. The chemical structures of the three polymers are provided in Scheme 1 and their characteristics are listed in Table 1. The photoacid generator, triphenylsulfonium perfluorobutanesulfonate (TPS-PFBS), was supplied by Toyo Gosei with chemical structure and follows the photolysis reaction as shown in Scheme 2. The deprotection reaction is shown in Scheme 3.

2.2. Sample preparation

Double-side polished, N-doped, high-resistivity silicon wafers with nominal thickness of 500 μm ± 25 μm were obtained from Nova Electronic Materials, Texas. A solution containing a mixture of polymer and TPS-PFBS (19:1 by mass) in cyclohexanone solvent (5% mass fraction) was spun coat on such wafers at a speed of 209 rad/s (2000 rpm) with an acceleration rate of 105 rad/s^2 (1000 rpm/s) for 60 s. The typical film thickness was approximately 150 nm as determined by X-ray reflectivity. The sample was post-apply baked at 130 °C for 60 s then exposed with a 248 nm broadband UV lamp. Different doses were produced by adjusting the exposure time on different areas of the wafer. The exposed samples were then transferred to a preheated hot-plate for post-exposure baking (PEB) immediately after exposure to minimize acid quenching by basic contaminants in the environment [11].

The effect of a single component on acid diffusion was tested using a multiple layer scheme. Bilayer samples consisting of an acid feeding layer and the protected polymer, PMAdMA, as a detection layer were used as reference samples. Trilayer samples were prepared with a layer of the component of interest located between the acid feeding layer and detection layer [12]. The feeding layer consists of poly(4-hydroxystyrene) with 5% mass fraction TPS-PFBS. The detection layer is the PMAdMA. The intermediate layer was either poly(methacrylic acid) (PMAA) or PGBLMA. Bilayer and trilayer films are prepared by utilizing the methods described earlier except that different solvents are used to ensure sharp interfaces between the layers.

2.3. FTIR spectroscopy

The extent of the deprotection reaction (shown in Scheme 3) and the amount of residual reaction product, methylene adamantane (MA), are measured with a Nicolet NEXUS 670 Fourier transform infrared (FTIR) spectrometer equipped with a liquid-nitrogen cooled Mercury Cadmium Telluride (MCT) detector. The data are collected in transmission mode with the OMNIC online-data acquisition software. A resolution of 8 cm^{-1} is used and 128 scans are averaged to improve the signal-to-noise ratio. With this resolution, the interference fringes produced by the double reflection of silicon wafer surfaces were greatly reduced without losing the spectroscopic features. Samples after PEB are directly transferred to a N_2 gas purged FTIR chamber at room temperature. No significant change in the deprotection level or MA residual level is observed when the sample is stored at room temperature for five days and/or under continuous N_2 purge for 15 min. The reaction-diffusion is effectively arrested at room temperature and the MA is trapped in the polymer matrix due to its high melting point (130 °C) and boiling point (203 °C).

[1] Certain equipment, instruments or materials are identified in this paper in order to adequately specify the experimental details. Such identification does not imply recommendation by the National Institute of Standards and Technology nor does it imply the materials are necessarily the best available for the purpose.

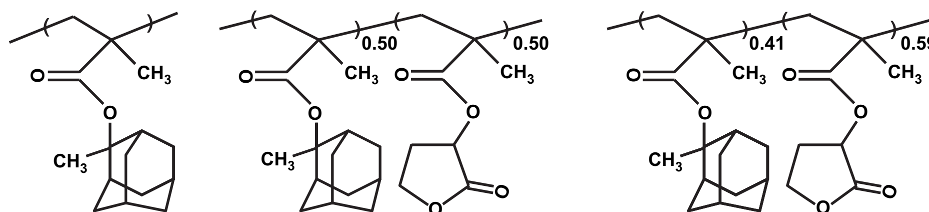

Scheme 1. Chemical structures of three photoresists used in this study; Left: PMAdMA; middle: P(MAdMA$_{50}$-*co*-GBLMA$_{50}$); right: P(MAdMA$_{41}$-*co*-GBLMA$_{59}$).

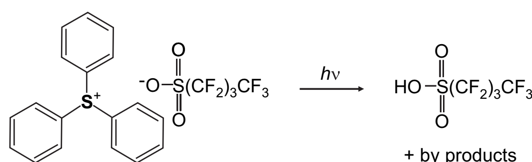

Scheme 2. Triphenylsulfonium perfluorobutanesulfonate (TPS-PFBS) photoacid generator and the corresponding photolysis reaction.

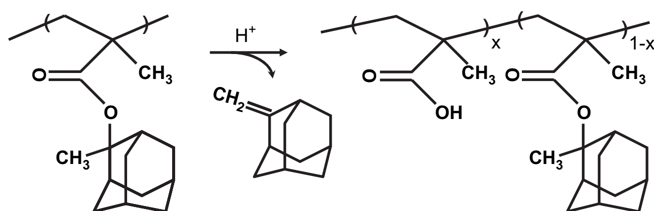

Scheme 3. Acid-catalyzed deprotection of PMAdMA.

Table 1
Polymer characteristics

Polymer	M_w	M_w/M_n	Glass transition temp. (°C)
PMAdMA	8800	1.18	>210
P(MAdMA$_{50}$-*co*-GBLMA$_{50}$)	12,800	1.67	161.9
P(MAdMA$_{41}$-*co*-GBLMA$_{59}$)	11,505	1.3	171.5

The deprotection reaction extent is quantified by the relative change in the area under the CH_3 bending vibration mode band of 1360 cm^{-1} in the protecting MA group of PMAdMA (Fig. 1a). This band completely disappears and leaves a flat baseline in the IR spectra when all the MA groups are reacted. Thus, this band provides an absolute value of deprotection extent and allows for the discrimination of free MA or residual MA from the protected MA group. In our experiments, only half of the wafer was exposed. Since the spin coated films are uniform across the wafer, the initial film thickness is the same for exposed and unexposed regions. The unexposed region is used as a reference and corrects for any difference in thickness between samples and avoids normalization problems. For the copolymers, this CH_3 band becomes too weak to obtain high quality data. Instead, a C–O stretching band (1260 cm^{-1}) is used (Fig. 1b). It should be noted that quantification with either band yields identical results. We have tested these two quantification methods with thicker films cast on KBr which provides stronger and higher resolution IR spectra for copolymer samples. The deprotection extent is identical irrespective of the choice of band used for quantification.

The quantification of MA residual level is based on the stretching vibration of H–C(=C) (3065 cm^{-1}) in the free MA molecule. This band is separated from other H–C(–C) vibration peaks (usually <3000 cm^{-1}), which allows quantification as shown in Fig. 2. Since pure MA is not commercially available, the direct calibration from IR absorbance of MA to its molar quantity is not possible. Instead, we use an indirect extrapolation method, where we assume that all MAs remain in the film when the deprotection or PEB time is close to zero.

3. Acid-catalyzed reaction model

The deprotection process in chemically amplified photoresists includes several steps: photoacid generation, photoacid diffusion, the catalyzed reaction with acid labile moieties, and the dissipation of methylene adamantane. A model is developed to quantify the reaction kinetics as a function of exposure dose, photoacid generator (PAG) loading, and other less examined factors such as products and copolymer composition. Acid diffusion is not included explicitly in the model because the precise mechanism and level of treatment of acid diffusion are varied [12–18]. The photoacid can be viewed as completely dissociated and diffuses as free ions in the polymer matrix. However, the size of photoacid counter anions is known to affect the diffusivity [15]. Generally, the acid diffuses cooperatively as one species with its conjugate base counteranion [15,16]. This assumption is appropriate for strong acids, such as perfluorobutanesulfonic acid. However, weaker acids are less dissociated in weakly polar or even non-polar polymer matrices [19]. The FTIR data over a range of processing conditions (exposure dose, temperature) can be fitted with the model to determine physically meaningful parameters such as the reaction rate constant.

The first step in the model is UV exposure that generates the photoacid. The concentration of photoacid can be calculated from the exposure dose by the following equation,

$$[\mathrm{H+}] = [\mathrm{PAG}]_0[1 - \exp(-CE)]. \quad (1)$$

where [H+] and $[\mathrm{PAG}]_0$ are the photoinitiated and initial PAG concentrations, respectively. E is the exposure dose and C is the Dill parameter that quantifies the efficiency of photolysis. Next, the acid diffuses through the polymer and catalyzes the deprotection reaction. As the reaction proceeds, protected

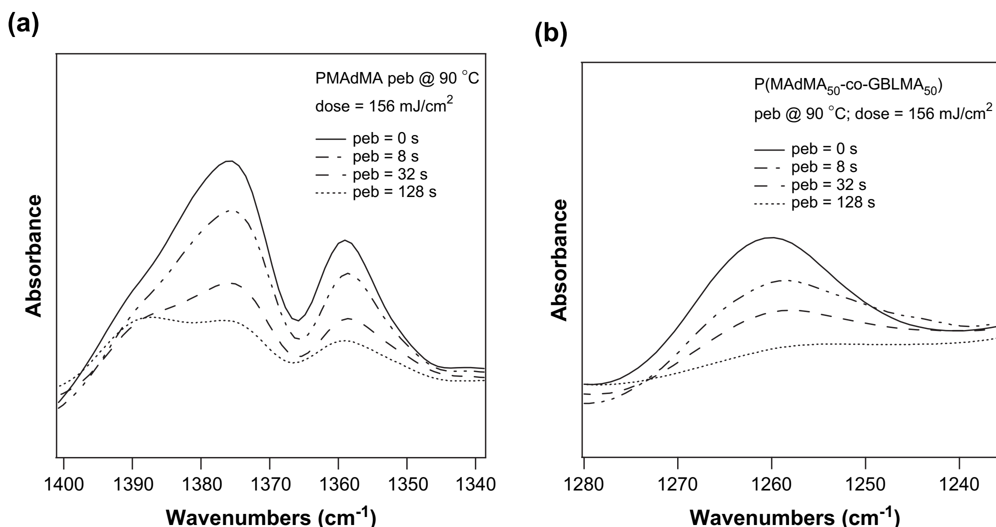

Fig. 1. The spectroscopic bands used for the characterization of deprotection level in PMAdMA (a) and copolymers (b).

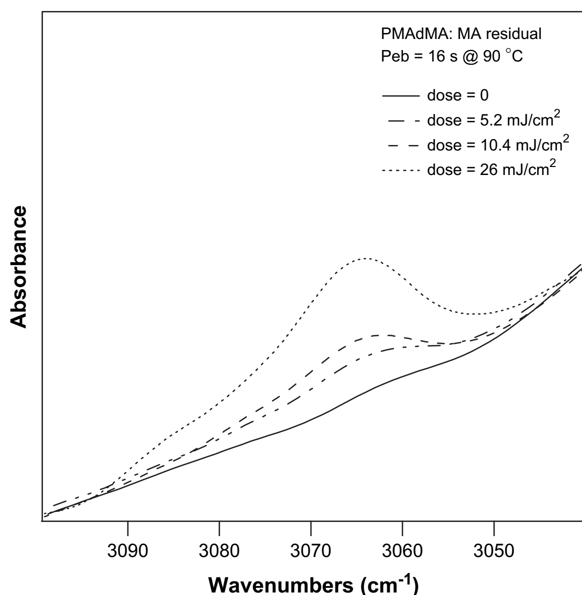

Fig. 2. Spectroscopic bands used for the quantification of residual MA inside the films.

groups are cleaved leading to a methacrylic acid (MAA) product as governed by Eq. (2).

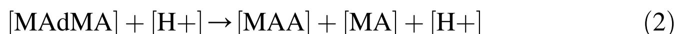

$$[\text{MAdMA}] + [\text{H}+] \rightarrow [\text{MAA}] + [\text{MA}] + [\text{H}+] \quad (2)$$

An auto-acceleration effect by the reaction products, reported for a hydroxystyrene system [19], was not observed in these experiments. This is consistent with the results from Paniez et al. [20], which use a similar methacrylate system.

To analyze the effect of the changing polymer matrix composition on the mobility of the photoacid, we assume that the system is homogeneous, i.e. the gradient of acid concentration is zero ($\partial[\text{H}+]/\partial x = 0$). The current approach on blanket exposed films is a special case of the conventional model [21]. It is difficult to model a variable diffusivity because the system must be treated heterogeneously as in the mesoscale simulation methods of Schmid et al. [5] or stochastic simulation methods of Houle et al. [13]. In some cases, the photoacid diffusion coefficient can vary by several orders in magnitude in protected versus deprotected polymers [12]. This appears as a reduced reaction rate in the presence of the deprotected polymer when the reaction is diffusion controlled [22]. In this system, the photoacid can be effectively trapped by MAA, implying that the diffusion coefficient becomes very small in MAA-rich regions leading to Eq. (3).

$$[\text{H}+] + [\text{MAA}] \rightarrow [\text{H}{-}\text{MAA}]_{\text{Trapped}} \quad (3)$$

this assumption is verified as will be discussed in greater detail.

A relationship was obtained by solving the two differential equations based on the above chemical reaction process,

$$\text{d}[\text{MAdMA}]/\text{d}t = -k_{\text{P}}[\text{H}+][\text{MAdMA}] \quad (4)$$

$$\begin{aligned}\partial[\text{H}+]/\partial t &= \partial/\partial x\,(D\partial[\text{H}+]/\partial x) - k_{\text{T}}[\text{MAA}][\text{H}+] \\ &= -k_{\text{T}}[\text{MAA}][\text{H}+] \end{aligned} \quad (5)$$

where the [MAdMA], [MAA] and [H+] are the molar concentrations of MAdMA, MAA and photoacid and D is the diffusion coefficient. For convenience, we use relative concentrations for MAdMA and MAA which are defined as their concentrations at time t relative to the initial MAdMA concentration, $[\text{MAdMA}]_0$. Since this is a time-independent constant, its insertion does not affect the above equations. In this approach, the reaction extent is dependent solely on the MAdMA component for both homopolymer and copolymers.

The k_{P} is the apparent acid catalysis reaction rate constant. Earlier investigations assumed that the acid-catalyzed reaction rate follows first-order kinetics in concentration of acid and reactant [19,22,23]. Zuniga and Neureuther found first-order reaction kinetics are unable to explain a nonlinear behavior of feature critical dimension on dose [24]. Despite the

different modeling approaches, it is generally agreed that the first-order kinetics cannot adequately describe the kinetics, especially at later reaction stages when the deprotection level is high. We demonstrate in Appendix that the reaction order is unity, verifying this assumption over the reaction conditions studied.

k_T is the apparent trapping rate constant for the acid. This acid loss factor was used by Petersen et al. to express the acid loss rate as first-order in acid concentration without an explicit dependence on the reaction extent [21,25]. These approaches consider all significant loss factors such as quenching by added bases, deprotection reactions, acid evaporation, as well as air-borne base contamination into one term, for simplicity. In the present study, we attribute an explicit first-order dependence on the reaction extent to consider the trapping of acid by the deprotection products as a primary physical mechanism. In commercial resist formulations the changes in deprotection extent are typically low to enhance resist sensitivity; therefore the acid loss factor would be pseudo-first order in acid concentration. Our study is not a general case, since it does not consider all acid quenching processes. The relatively short reaction times and large changes in deprotection extent observed with these model materials require an acid loss rate dependence on the deprotection extent. This approach provides an interpretation for the observed reaction slowdown effect at high deprotection extents.

Conventionally, this reaction slowdown is modeled with a variable diffusivity [26,27]. However, introduction of this trapping factor can incorporate effects from both acid loss and diffusivity change. This model does not necessarily generate better fits to the data, but does provide a reasonable explanation about the reaction-diffusion behavior with fewer parameters. It is also possible to use forward and reverse reaction constants to model the trapping behavior. In the present case, this approach is not necessary because of the large contrast in the diffusion coefficient between PMAdMA and reaction product PMAA.

The deprotection level (ϕ) can be calculated from the relative molar concentration of MAdMA groups.

$$\phi \equiv 1 - [\text{MAdMA}]/[\text{MAdMA}]_0 = [\text{MAA}]/[\text{MAdMA}]_0 \qquad (6)$$

rearranging the above equations and solving for [H+] results in the following expression:

$$[\text{H+}] = [\text{H+}]_0 + k_T/k_P[\text{MAdMA}]_0[\phi + \ln(1-\phi)] \qquad (7)$$

$$\text{d}\phi/\text{d}t = k_P[\text{H+}](1-\phi) \qquad (8)$$

where $[\text{H+}]_0$ is the initial photoacid concentration determined by Eq. (1). The deprotection level is calculated by combining Eqs. (1), (7) and (8). Therefore by fitting these equations into the data, we determine the Dill parameter (C), the apparent reaction constant (k_P) and the acid-trapping factor (k_T). By fitting the data from several exposure doses, this approach provides independent verification of the reaction rate constants and improves confidence in the results. The experimental data were fit to the model using a least-squares regression routine. The deprotection level defined in this way also applies for copolymers because only the MAdMA functional groups take part in the reaction. The initial number density of MAdMA requires adjustment to account for the comonomer dilution as summarized in Table 2. The fitting parameters for the three copolymers examined are listed in Table 3. Details regarding photoacid concentration and Dill parameters can be found in Appendix.

4. Results and discussion

4.1. Homopolymer: varying dose and temperature

Fig. 3a shows the time evolution of the deprotection level at varying exposure doses and 130 °C post-exposure bake temperature for the PMAdMA resist containing TPS-PFBS. The solid lines are fit to the data using the chemical reaction kinetics model discussed earlier. The deprotection level increases with dose and PEB time as expected. For doses of 26 mJ/cm^2 and higher, there are no differences in the final deprotection level because these doses are sufficient for complete photolysis of the PAG. At lower doses, (5.2 and 10.4) mJ/cm^2, the initial reaction rate has decreased as seen from the smaller slope and significantly longer bake times are needed for reaction completion. The quantitative effect will be determined by the model, however, the overall reduced average level of deprotection is persistent at low doses or low photoacid concentration. This effect is not simply due to a lower concentration of reactants. Fig. 3b and c shows the results from lower reaction temperatures of 110 °C and 90 °C, respectively. The trends are similar to the results at 130 °C especially the persistence of low deprotection extents at low doses, signifying that the reaction rate is suppressed.

Table 2
Resist compositional characteristics

Polymer resists	Mass fraction of MAdMA	Density (ρ)[a] (g cm^{-3})	$[\text{PAG}]_0$ (nm^{-3})[b]	$[\text{MAdMA}]_0$ (nm^{-3})[c]
PMAdMA	1	1.13	0.061	2.86
P(MAdMA$_{50}$-*co*-GBLMA$_{50}$)	0.577	1.20	0.065	1.75
P(MAdMA$_{41}$-*co*-GBLMA$_{59}$)	0.487	1.23	0.067	1.52

ρ is the mass density of polymer resists, M_o is the repeat unit molecular weight, ε is the mass fraction of MAdMA in a polymer chain and N_A is the Avogadro's constant.
[a] The film density values were determined by X-ray reflectivity.
[b] $[\text{PAG}]_0 = 0.05\,\rho\,N_A/M_{o,\text{PAG}}$.
[c] $[\text{MAdMA}]_0 = \varepsilon\,\rho\,N_A/M_{o,\text{MAdMA}}$.

Table 3
Summary of reaction kinetics parameters

Experiments	Temp. (°C)	C (cm^2/mJ)	k_P (nm^3 s^{-1})	k_T (nm^3 s^{-1})
PMAdMA	90	0.028	0.95	0.016
PMAdMA	110	0.022	17.4	0.073
PMAdMA	130	0.021	31.8	0.112
P(MAdMA$_{50}$-*co*-GBLMA$_{50}$)	90	0.028	0.50	0.015
P(MAdMA$_{50}$-*co*-GBLMA$_{50}$)	110	0.018	9.7	0.114
P(MAdMA$_{41}$-*co*-GBLMA$_{59}$)	110	0.050	2.0	0.100

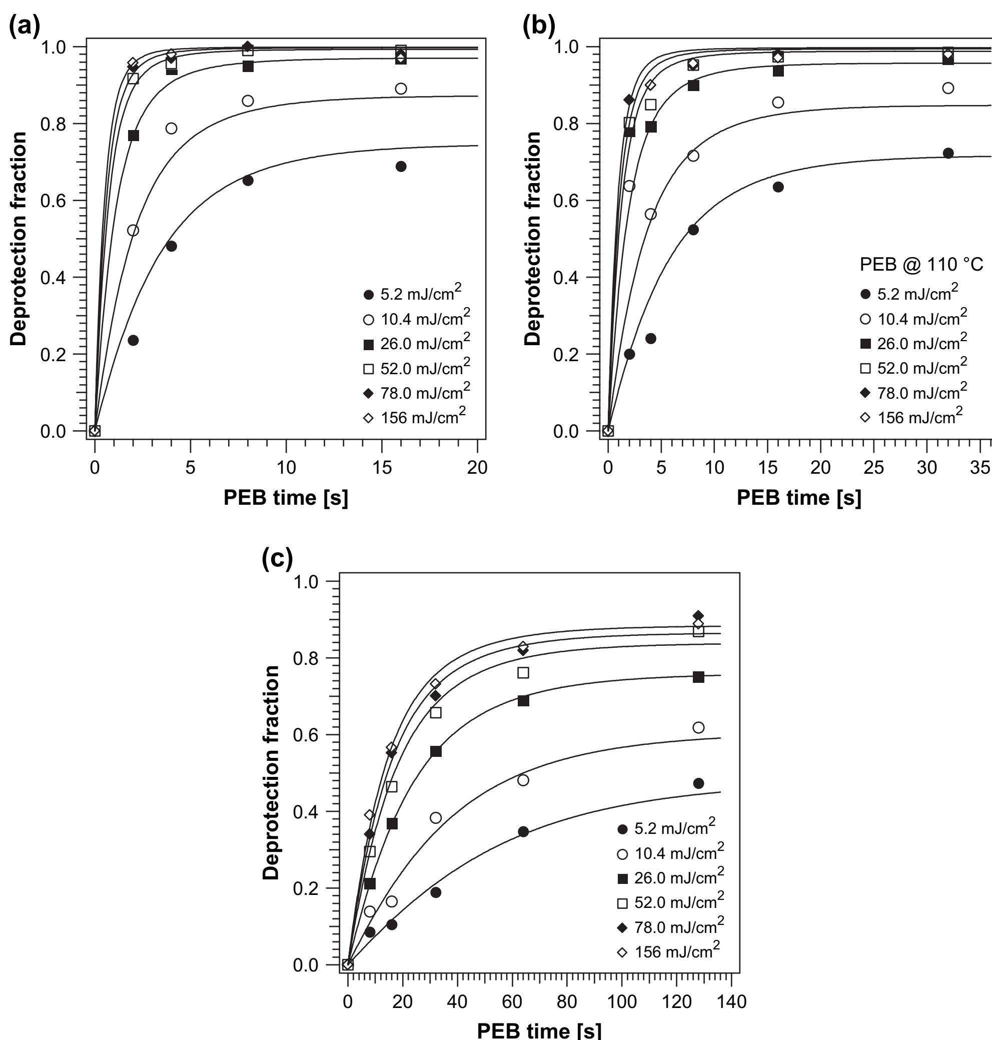

Fig. 3. The deprotection level versus post-exposure bake time for PMAdMA containing 5.0% TPS-PFBS photoacid generator at three temperatures (a) 130 °C, (b) 110 °C, and (c) 90 °C. Several doses 5.2, 10.4, 26, 52, 78 and 156 mJ/cm^2 were applied as given in the legend. The lines are drawn by fitting the data to the model mentioned in the text.

In many cases, the deprotection products are highly volatile and a rapid outgassing is followed by a volume relaxation of the polymer film [28]. The methylene adamantane products in this system are relatively large and were expected to lead to limited outgassing. Fig. 4 shows the evolution of methylene adamantane within the film for a PEB temperature of 90 °C. The open circles are the ideal concentrations calculated from the measured extent of reaction, whereas the open squares are the actual MA contents. In addition to the deprotection reaction, the local environment of the photoacid is affected by the formation and loss of the MA reaction product. The MA concentration in the film first increases and then decreases with increasing reaction time. At early times, the deprotection reaction is rapid and the methylene adamantane content increases. At longer times, the deprotection reaction slows down and the rate of MA evaporation becomes larger than the MA production rate. The MA content decreases continuously, even at temperatures below the reported melting point of pure MA, 136 °C [29]. The loss of MA does result in a change in volume and could affect the deprotection reaction kinetics from an increase in the concentration of the reacting species in the sample. The Chemical Kinetics Simulator [30] was used to consider the effect of volume changes during the reaction on the reaction kinetics of a bulk system. Simulations were performed following the approach of Wallraff et al. [19]; one result is shown in Fig. 5. The volume change in this system does not play a significant role in the reaction kinetics.

4.2. Copolymer: varying dose and composition

Fig. 6a and b shows the time evolution of extent of deprotection for two copolymer resists containing 50 mol% GBLMA and 59 mol% GBLMA at a PEB temperature of 110 °C. Similar to the homopolymer, the initial reaction rate is strongly dependent on the photoacid concentration or exposure dose. The reaction rate decreases at longer times and then levels off at late deprotection stages. As the GBLMA content increases, the reaction rate decreases. This result is partially due to the lower reactant (MAdMA) concentration, however, the interaction of the GBLMA with the acid is also important

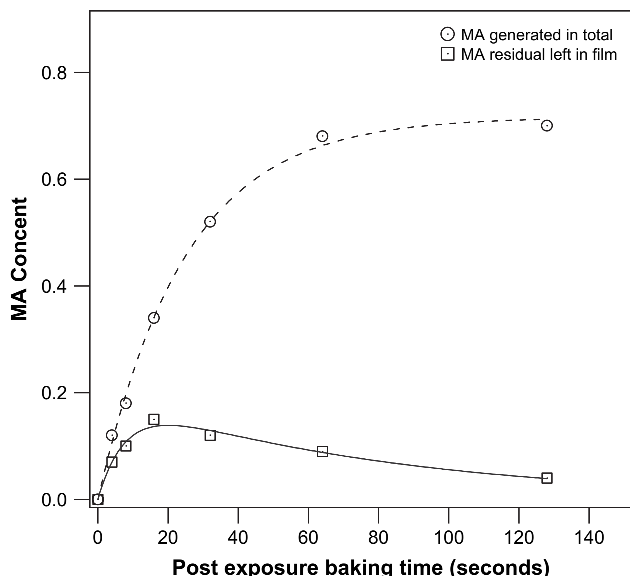

Fig. 4. The MA residual content measured with FTIR for a PMAdMA resist single layer with 2.0% PFBS loading (exposure dose: 156 mJ/cm^2; PEB temperature: 90 °C). The MA content is defined as the molar ratio of MA free molecules to the initial MAdMA moiety in the sample. The total MA content, if confined inside the sample, is equal to the deprotection level. The lines are drawn to guide the reader's eye.

as will be discussed later. For copolymer samples, the deprotection level is defined as the relative conversion ratio of MAdMA to the total polymer resist system; therefore the diluting factor due to copolymer composition has been excluded automatically.

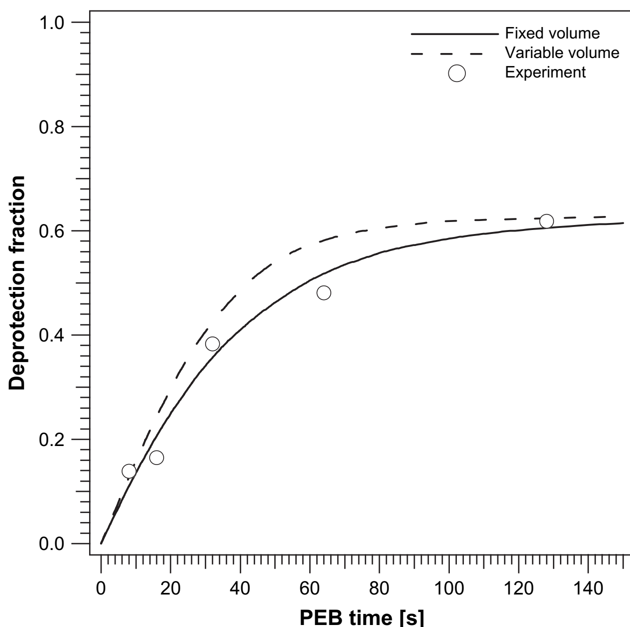

Fig. 5. Chemical Kinetics Simulations results for PMAdMA processed at 90 °C with dose of 5.2 mJ/cm^2. The solid line describes the reaction kinetics curve if the methylene adamantane is assumed to be a gas. The dotted line is the model with no volume change. Since methylene adamantane is a low-volatility solid, only partial loss occurs. The true reaction kinetics curve should fall between these two limits. Therefore we conclude that volume change does not appear to significantly influence the reaction kinetics.

4.3. Acid-catalyzed reaction rate

As the GBLMA content increases, the apparent reaction rate constant, k_P, decreases as shown in Fig. 7. For an ideal fully homogeneous chemical reaction condition, this result would be unusual because the reaction constant should not change with the reactant concentration, only the reaction rate should change. However, this apparent rate constant includes the effects of photoacid strength, diffusivity [22] and resist polarity [31]. Since the photoacid strength is fixed, the trends in the reaction constants are due to changes in the acid diffusivity and changes in the composition of the thin film. These two factors are correlated because the acid diffusivity can be reduced through strong and specific interactions with the polymer. The interaction of the polymer matrix with the photoacid is enhanced by the substitution of non-polar MAdMA groups with polar GBLMA groups. The carbonyl group of GBLMA and the acrylate on the main chain can serve as a hydrogen-bond acceptor. One example is shown in Fig. 8 for unexposed and exposed-baked 50 mol% GBLMA copolymer. The band at 1790 cm^{-1} is associated with the lactone in GBLMA and broadens after PEB due to hydrogen bonding with PMAA, with C═O at 1740 cm^{-1}. Since the photoacid is a much stronger acid than PMAA, we expect that GBLMA could also hydrogen bond with photoacid. However, with the current data it is not possible to differentiate PMAA or photoacid due to the weak signal from the dilute photoacid. In a different system, Lee et al. [32] showed that the diffusion coefficients of probe molecules were greatly reduced by hydrogen bonding interactions with a polymer in solution.

To confirm that strong interaction between the GBLMA moiety and the photoacid can affect the acid diffusivity, we performed bilayer and trilayer experiments [12]. The detection layer is sensitive enough in such a way that the reaction is immediately detected once the diffusing photoacid arrives. When the acid feeding layer is in direct contact with PMAdMA, (50–70)% deprotection can occur within (8–15) s [10]. In this case, there is no barrier to the acid diffusion. When an intermediate layer of PGBLMA is used in a trilayer configuration, (120–240) s are required to achieve similar deprotection levels at identical reaction conditions. The film thickness of the intermediate layer is comparable with the detection layer, so the diffusion coefficient of photoacid in PGBLMA is estimated to be approximately one order of magnitude (8–30×) smaller than that through PMAdMA. The diffusivity of photoacid is clearly reduced by the presence of GBLMA. We note that the effect of local composition fluctuations in the GBLMA layer on the trajectory of the photoacid can only be captured through heterogeneous modeling [2]. A quantitative relationship between photoacid diffusivity and the apparent reaction constant was proposed by Nakamura et al. [33]. They proposed that the observed reaction rate constant is proportional to the diffusion coefficient of photoacid and the resist reaction probability per photoacid. In the case of fixed acid cleavable group chemistry, the reaction probability will be independent of polymer composition. Thus, the observed reduction in k_P with

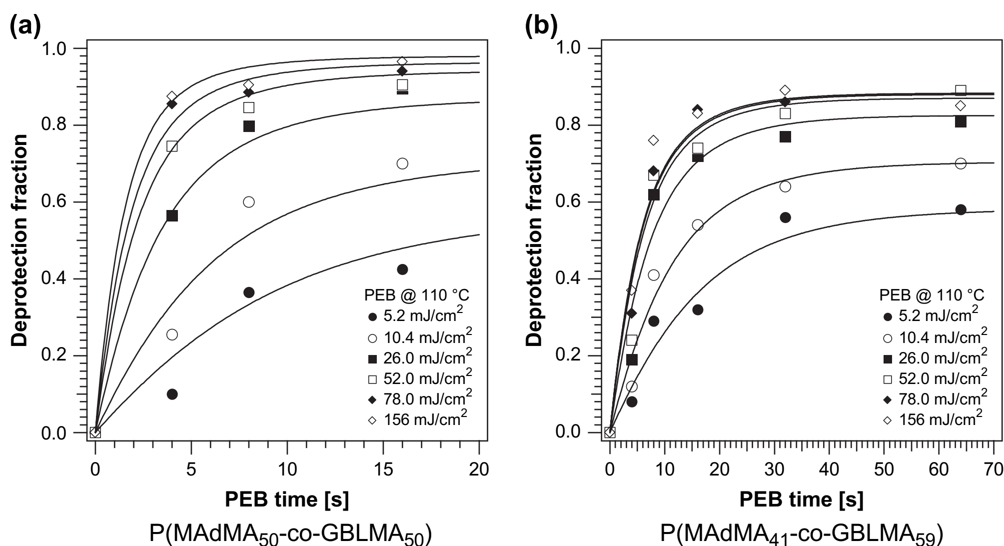

Fig. 6. The absolute molar deprotection level versus post-exposure bake time for the resist copolymers: (a) P(MAdMA$_{50}$-*co*-GBLMA$_{50}$) and (b) P(MAdMA$_{41}$-*co*-GBLMA$_{59}$) containing 5.0% by mass TPS-PFBS photoacid generator processed at 110 °C. The dose is provided in the legend. The model fitted lines are also shown.

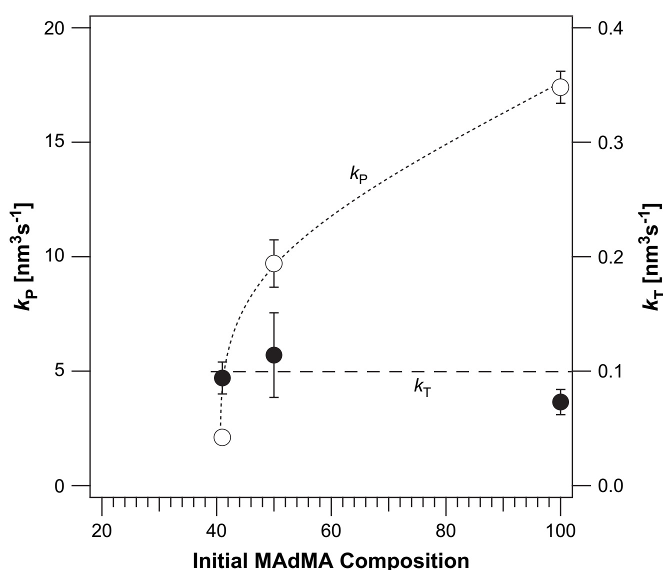

Fig. 7. Summary of the rate constants for acid catalysis (k_P) and apparent acid trapping (k_T) as a function of the methyladamantyl protecting group content at PEB temperature of 110 °C. The lines are drawn for guiding the eye. The error bar is corresponding to one standard deviation of uncertainty obtained by fitting the kinetics data with regression model.

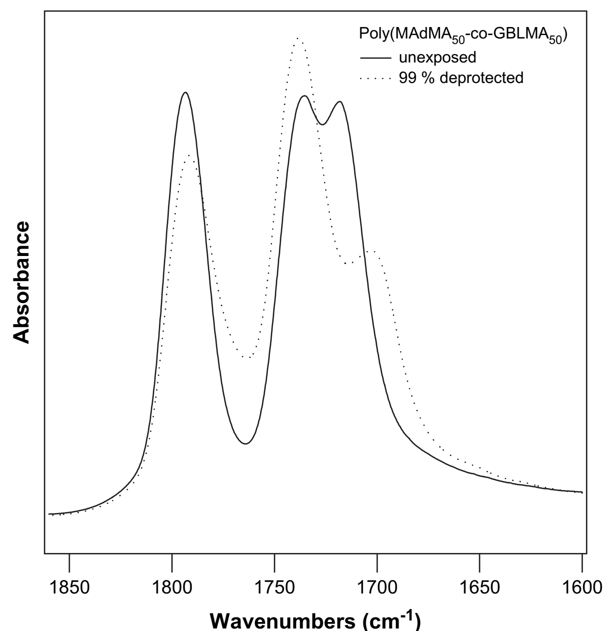

Fig. 8. Spectroscopic band at 1790 cm^{-1} is associated with C=O group in the lactone of GBLMA and broadens after PEB due to hydrogen bonding.

increasing GBLMA content is consistent with a reduced photoacid diffusivity.

4.4. Acid trapping

As the reaction proceeds and the deprotection products increase in local concentration, the reaction rate decreases. This observation could be interpreted as acid loss [8,21,23–25], a variable diffusion coefficient [15,26,34], or a changing reaction order [24]. The FTIR data confirm that the reaction order for this system is one (see Appendix). For this system, the FTIR data are fit with a model that includes an acid-trapping or self-quenching rate constant (k_T). The results are summarized in Table 3 and plotted in Fig. 7. The trapping rate constant is found to be independent of the initial copolymer fraction. Therefore, the non-reactive lactone moiety is not responsible for this rate constant. In addition, this trapping rate constant is different from other suggested loss factors which are linear in photoacid concentration and independent of resist composition [8,21]. The most consistent explanation for the trapping rate constant is through a reduced diffusivity that is sufficiently low that the photoacid appears inactive.

This only occurs as the deprotection product increases in local concentration through the first-order reaction (Eq. (3)).

To demonstrate the reduced diffusivity of the photoacid, a trilayer sample was prepared with poly(methacrylic acid) (PMAA) as the intermediate layer. Following the same exposure and bake conditions as the GBLMA study, no deprotection reaction was detected after 1 h. Therefore, the diffusion rate of the photoacid in poly(methacrylic acid) or methacrylic acid rich regions is extremely low when compared with the diffusivity of the acid in protected polymers over the time scale of a typical reaction (less than 3 min). We note that the reaction temperatures are well below the glass transition temperature of these polymers. The trapping of the acid could reflect the slower dynamics of the polymer matrix. The free volume in the polymers is expected to be relatively independent of polymer types and should be approximately constant [35]. Nevertheless, the apparent reaction rate constant appears to be inconsistent with the glass transition temperature of each copolymer. For instance, the PMAdMA has a higher glass transition temperature than the 50 mol% GBLMA copolymer, yet the reaction rate is a factor 8.7 larger even though the process temperatures are nearly 100 °C and 50 °C below the nominal glass transition as shown in Table 1. It is not clear how many methacrylic acid units are necessary to trap one photoacid. However, this model with a first-order reaction in terms of the MAA and photoacid concentration, and k_T characterizing the acid-trapping rate is sufficient to fit the data.

Since GBLMA is also a hydrogen-bond acceptor, it could contribute to a trapping reaction. However, the GBLMA content is a constant with reaction time and would appear as a constant factor within k_T in the model developed here. The data in Table 3 do not show a dependence with increased GBLMA content. Therefore, the rate constant for this reaction is rate-limited by the PMAA trapping step. A model that would include the effect of the GBLMA moieties would include a reversible step as suggested by the relatively higher diffusivity of the acid in GBLMA than in PMAA. This result shows that influence of the GBLMA on both reaction and diffusion into k_P remains physically plausible. Extensions to other chemical functional groups, other than GBLMA, may require more than one trapping step. These considerations are well suited for the simulation approaches described earlier.

5. Conclusion

The deprotection reaction kinetics in model photoresists is influenced by the copolymer composition and reaction products. A chemical reaction kinetics model was developed to describe the dependence of the deprotection level on reaction time and photoacid concentration. Through this model, we find that the deprotection reaction rate constant decreases with increased lactone content. This change is attributed to a systematic decrease in the photoacid diffusivity due to hydrogen bonding with the polar groups in the gammabutyrolactone functional groups. Similarly, the slowing down of the reaction rate at high deprotection extents can be understood through hydrogen bonding between photoacid and the methacrylic acid groups. These observed relationships between the deprotection reaction kinetics and the polymer microstructure highlight processes that must be included in future reaction-diffusion experimentation and modeling.

Acknowledgements

This work was supported by SEMATECH under Agreement #: 309841 OF. The authors acknowledge M. Padmanaban and Ralph Dammel at AZ Electronics and Jim Sounik and Michael Sheehan at DuPont Electronic Polymers for providing the polymers used in this study.

Appendix

A.1. Photoacid concentration and Dill parameter

The photo acid concentration is calculated from Dill's parameter, the dose and the initial PAG loading. The method assumes the PAG is completely converted after the dose reaches saturation. Previously, Houle and coworkers [13] measured the conversion efficiency of photoacid generated by PFBS under irradiation at 254 nm using a titration method and found nearly 87% efficiency for a 1180 nm thick film. Considering potential absorption, the efficiency should be greater for the 140 nm thick PMAdMA film used in this study. The Dill parameter measured for different process temperatures and polymer systems are in good agreement. This is expected, since the Dill parameter relates to the photolysis mechanism

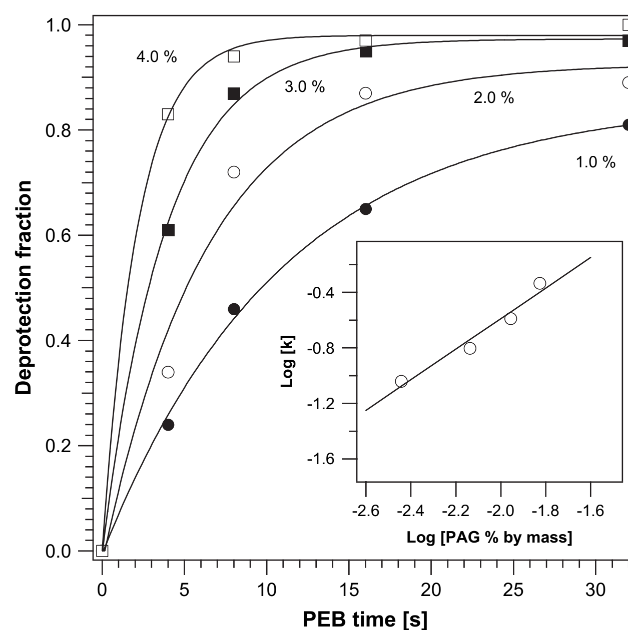

Fig. 9. Reaction kinetics determined by FTIR for P(MAdMA$_{50}$-*co*-GBLMA$_{50}$) as a function of TPS-PFBS loading indicated on the plot for a PEB of 110 °C with 356 mJ/cm^2 dose. The curves are fitted lines according to the above model. Inset: the reaction order is determined by the slope on a log−log plot of rate constant versus PAG loading, $m = 1.10 \pm 0.20$.

and irradiation source. However, the measured Dill parameter can be influenced by polymer absorption. The anomaly for the P($MAdMA_{41}$-*co*-$GBLMA_{59}$) polymer is not clear, but may be related to synthetic preparation of the polymers.

A.2. Reaction order verification

A simple method of estimating the reaction order for these thin films is possible by using high dose to photoinitiate all PAG and vary the PAG concentration in a systematic manner. Fig. 9 shows the experimental data for 1, 2, 3, and 4% by mass PAG loadings. If the reaction is written as $d\phi/dt = k\,[H+]^m\,(1-\phi)$, the reaction order "$m$" can be found by assuming that the corresponding self-trapping behavior is negligible at high dose/loadings which is the limit we investigate, confirmed by the small ratio of k_T/k_P. The exponent "m" can be measured since the acid-trapping factor k_T is relatively small compared to the reaction constant k_P, we can ignore the change in photoacid concentration due to the trapping. Therefore, the exponential form of the deprotection level versus PEB time is fit and m is obtained from the logarithm of the time constant (τ) versus logarithm of [PAG]: $\log(\tau) = A + m\log([PAG])$, where "$A$" is a constant independent of [PAG]. The m was found to be 1.10 ± 0.20 by fitting the above equation into the data. Therefore, first-order kinetics is a reasonable assumption in our system.

References

[1] Ito H. Advances in Polymer Science 2005;172:37–245.
[2] Houle F, Hinsberg WD, Sanchez M, Wallraff G, Larson C, Hoffnagle J. Journal of Vacuum Science and Technology B 2000;18:1874–85.
[3] Postnikov SV, Stewart MD, Tran HV, Nierode MA, Medeiros DR, Cao T, et al. Journal of Vacuum Science and Technology B 1999;17:3335–8.
[4] Lin EK, Soles CL, Goldfarb DL, Trinque BC, Burns SD, Jones RL, et al. Science 2002;297:372–5.
[5] Schmid GM, Stewart MD, Singh VK, Willson CG. Journal of Vacuum Science and Technology B 2002;20:185–90.
[6] Hinsberg W, Houle FA, Hoffnagle J, Sanchez M, Wallraff G, Morrison M, et al. Journal of Vacuum Science and Technology B 1998;16:3689–94.
[7] Houle FA, Hinsberg WD, Sanchez MI. Journal of Vacuum Science and Technology B 2004;22:747–57.
[8] Nagahara S, Yuan L, Poppe WJ, Neureuther A, Kono Y, Sekiguchi A, et al. Proceedings of SPIE 2005;5753:338–49.
[9] Krautter H, Houlihan F, Hutton R, Rushkin I, Opila R. In: Proceedings of the SPIE. Advances in resist technology and processing XVII, vol. 3999; 2000. p. 1070–8.
[10] Vogt BD, Kang SH, Prabhu VM, Lin EK, Satija SK, Turnquest K, et al., submitted for publication.
[11] Hinsberg WD, Macdonald SA, Clecak NJ, Snyder CD. Chemistry of Materials 1994;6:481–8.
[12] Postnikov SV, Stewart MD, Tran HV, Nierode MA, Medeiros DR, Cao T, et al. Journal of Vacuum Science and Technology B 1999;17:3335–8.
[13] Houle FA, Hinsberg WD, Morrison M, Sanchez MI, Wallraff G, Larson C, et al. Journal of Vacuum Science and Technology B 2000;18:1874–85.
[14] Itani T, Yoshino H, Fujimoto M, Kasama K. Journal of Vacuum Science and Technology B 1995;13:3026–9.
[15] Stewart MD, Tran HV, Schmid GM, Stachowiak TB, Becker DJ, Willson CG. Journal of Vacuum Science and Technology B 2002;20:2946–52.
[16] Shi X. Journal of Vacuum Science and Technology B 1999;17:350–4.
[17] Berger CM, Henderson CL. Proceedings of SPIE 2004;5376:392–403.
[18] Nakamura J, Ban H, Tanaka A. Journal of Vacuum Science and Technology B 1992;12:3888–94.
[19] Wallraff G, Hutchinson J, Hinsberg WD, Houle FA, Seidel P, Johnson R, et al. Journal of Vacuum Science and Technology B 1994;12:3857–62.
[20] Paniez P, Gally S, Mortini B, Rosilo C, Sassoulas P-O, Dammel RR, et al. In: Proceedings of the SPIE. Advances in resist technology and processing XVI, vol. 3678; 1999. p. 1352.
[21] Petersen JS, Mack CA, Thackeray JW, Sinta R, Fedynyshyn TH, Mori JM, et al. Proceedings of SPIE 1995;2438:153.
[22] Nakamura J, Ban H, Tanaka A. Japanese Journal of Applied Physics 1992;31:4294–300.
[23] Krasnoperova AA, Khan M, Rhyner S, Taylor JW, Zhu Y, Cerrina F. Journal of Vacuum Science and Technology B 1994;12:3900–4.
[24] Zuniga M, Neureuther A. Journal of Vacuum Science and Technology B 1995;13:2957–62.
[25] Byers JD, Petersen JS, Sturtevant J. Proceedings of SPIE 1996;2724:156.
[26] Yuan L, Neureuther A. Proceedings of SPIE 2003;5039:1041.
[27] Petersen JS, Byers JD. Proceedings of SPIE 1996;2724:163.
[28] Wallraff G, Hutchinson J, Hinsberg W, Houle F, Seidel P, Johnson R, et al. Journal of Vacuum Science and Technology B 1994;12:3857–62.
[29] Bakker B, Cerfontain H, Tomassen P. Journal of Organic Chemistry 1989;54:1680–4.
[30] Chemical Kinetics Simulator program package is available for a no-cost license from IBM at http://www.almaden.ibm.com/st/msim/; 2005.
[31] Pohlers G, Barclay G, Stafford C, Barbieri T, Cameron J. In: Proceedings of the SPIE. Advances in resist technology and processing XXI, vol. 5376; 2004. p. 79–93.
[32] Lee J, Park K, Chang T, Jung J. Macromolecules 1992;29:6977–9.
[33] Nakamura J, Ban H, Tanaka A. Japanese Journal of Applied Physics Part 1 – Regular Papers Short Notes and Review Papers 1992;31:4294–300.
[34] Petersen JS, Mack CA, Sturtevant J, Byers JD, Miller DA. Proceedings of SPIE 1995;2438:167.
[35] Young RJ, Lovell PA. Introduction to polymers. 2nd ed. Stanley Thornes Ltd.; 1991.